ACS SyntheticBiology

Letter

pubs.acs.org/synthbio

Red Light-Regulated Reversible Nuclear Localization of Proteins in Mammalian Cells and Zebrafish

Hannes M. Beyer,[¶,†,‡,§] Samuel Juillot,[¶,†,‡,§] Kathrin Herbst,[¶,∥,⊥] Sophia L. Samodelov,[†,‡,§] Konrad Müller,[†] Wolfgang W. Schamel,[†,‡,§,#] Winfried Römer,[†,‡,§] Eberhard Schäfer,[†] Ferenc Nagy,[†,▽] Uwe Strähle,[∥] Wilfried Weber,[†,‡,§,⊗] and Matias D. Zurbriggen*[,†,‡]

[†]Faculty of Biology, University of Freiburg, Schänzlestrasse 1, 79104 Freiburg, Germany

[‡]BIOSS – Centre for Biological Signalling Studies, University of Freiburg, Schänzlestrasse 18, 79104 Freiburg, Germany

[§]SGBM – Spemann Graduate School of Biology and Medicine (SGBM), University of Freiburg, Albertstrasse 19a, 79104 Freiburg, Germany

[∥]Institute of Toxicology and Genetics, Karlsruhe Institute of Technology and University of Heidelberg, D-76344 Eggenstein-Leopoldshafen, Germany

[⊥]BIF-IGS – BioInterfaces International Graduate School, Hermann-von-Helmholtz-Platz 1, 76344 Eggenstein-Leopoldshafen, Germany

[#]CCI, Centre for Chronic Immunodeficiency, University Clinincs Freiburg, Breisacher Strasse 117, 79106 Freiburg, Germany

[▽]Biological Research Centre, Institute of Plant Biology, H-6726 Szeged, Hungary

[⊗]ZBSA – Centre for Biosystems Analysis, University of Freiburg, Habsburgerstrasse 49, 79104 Freiburg, Germany

Supporting Information

ABSTRACT: Protein trafficking in and out of the nucleus represents a key step in controlling cell fate and function. Here we report the development of a red light-inducible and far-red light-reversible synthetic system for controlling nuclear localization of proteins in mammalian cells and zebrafish. First, we synthetically reconstructed and validated the red light-dependent *Arabidopsis* phytochrome B nuclear import mediated by phytochrome-interacting factor 3 in a nonplant environment and support current hypotheses on the import mechanism *in planta*. On the basis of this principle we next regulated nuclear import and activity of target proteins by the spatiotemporal projection of light patterns. A synthetic transcription factor was translocated into the nucleus of mammalian cells and zebrafish to drive transgene expression. These data demonstrate the first *in vivo* application of a plant phytochrome-based optogenetic tool in vertebrates and expand the repertoire of available light-regulated molecular devices.

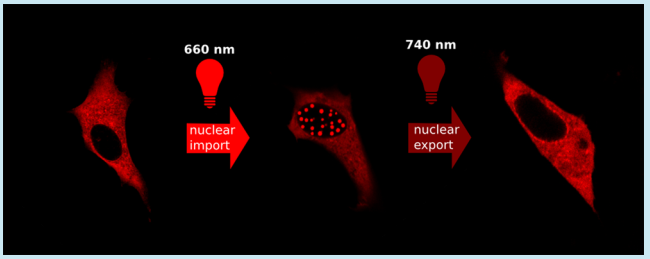

KEYWORDS: *light-inducible nuclear transport, optogenetics, phytochrome, mammalian synthetic biology, plant synthetic biology*

Entry and exit of proteins into and out of the nucleus represents a key signaling step regulating cell fate and function. Signals originating from membrane-bound or intracellular receptors are transduced *via* signaling cascades to final control steps in which transcription factors are translocated to the nucleus to orchestrate the expression of target genes. These cascades govern essential processes such as the development and differentiation of cells to organs,[1] tissue regeneration and homeostasis,[2] and the development and activation of immune cells.[3] Moreover, the deregulated nuclear localization of signaling proteins is associated with major diseases, including cancer.[4,5] The detailed qualitative and quantitative characterization of key cellular processes in basic and applied research is based on the availability of molecular tools to exogenously stimulate or inhibit signal transduction.

The recent advent of optogenetics has provided a toolset for the precise manipulation and understanding of signaling processes with unmatched spatiotemporal resolution. Having originally emerged in neurobiology with the optical stimulation of neural cells, recent research in photobiology and synthetic biology has yielded optogenetic tools to render diverse cellular processes responsive to light.[6,7] Examples include light-regulated membrane recruitment,[8,9] light-responsive kinase[10] and protease[11] activities, UV-controlled protein secretion,[12] the retention of proteins in cellular compartments,[13−15] protein stability,[16] and protein clustering[17] or caging.[11,18] Moreover, functionally orthogonal tools for differentially controlling the

Received: January 9, 2015
Published: March 24, 2015

DOI: 10.1021/acssynbio.5b00004
ACS Synth. Biol. 2015, 4, 951−958

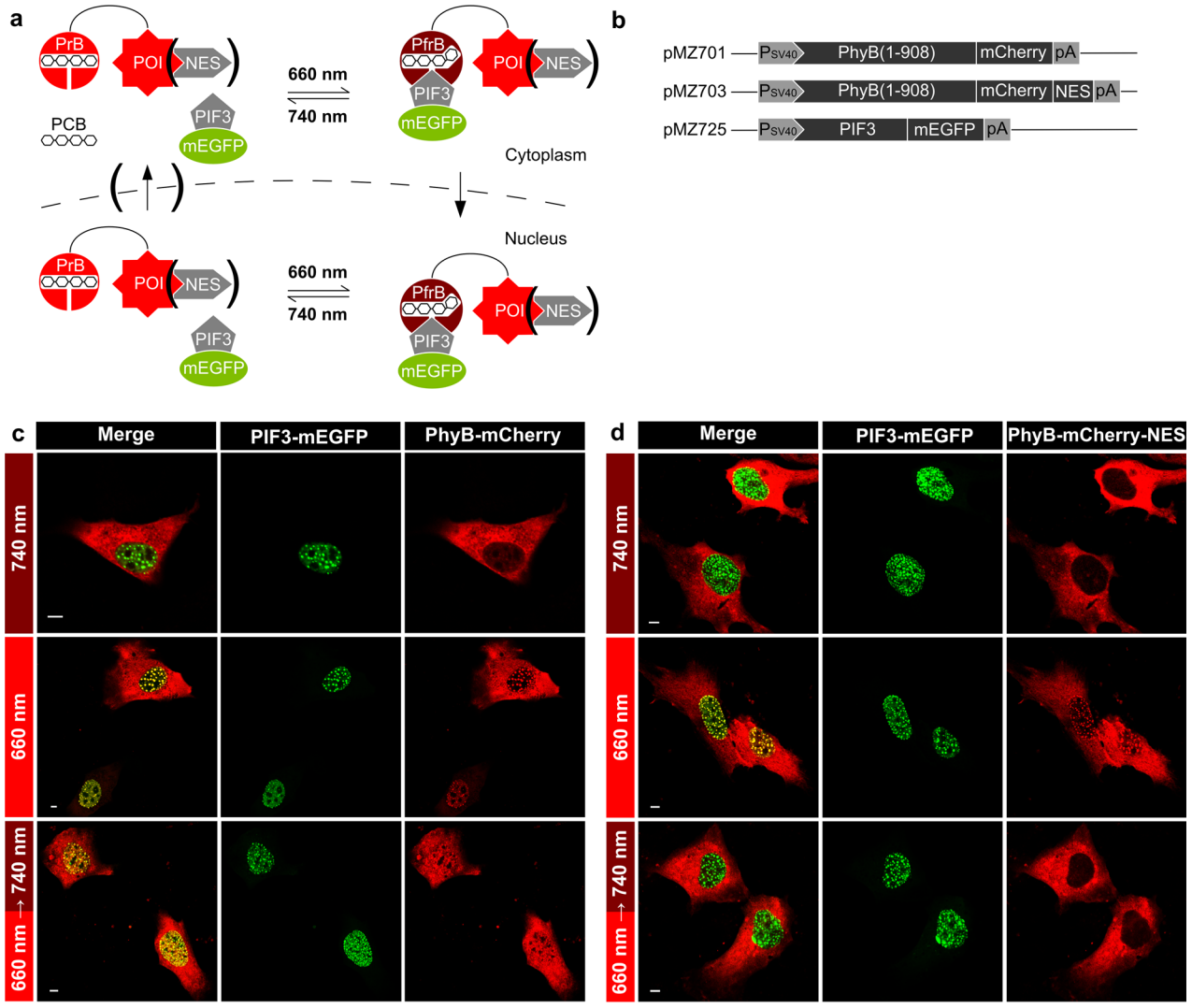

Figure 1. Red light-inducible, far-red light-reversible nuclear localization of proteins. (a) Design of the red light-controlled nuclear localization system. *Arabidopsis* phytochrome B (PhyB, amino acids 1−908) is fused to the protein of interest (POI) and optionally to a nuclear export signal (NES). Upon illumination with red light (660 nm), PhyB is converted to the Pfr state (PfrB) and binds full-length phytochrome-interacting factor 3 (PIF3) harboring an intrinsic nuclear localization signal (NLS) to mediate nuclear transport of the heteromeric protein complex. Upon illumination at 740 nm, PhyB is converted to the Pr state (PrB) leading to the dissociation of PIF3. In the presence of an NES, PhyB is shuttled back to the cytoplasm, whereas in the absence of an NES PhyB remains in the nucleus. (b) Expression cassettes for the red light-inducible nuclear localization system. (c) Red light-inducible nuclear localization of proteins. NIH/3T3 cells were cotransfected with expression vectors pMZ701 and pMZ725. Twenty-four hours post transfection, the medium was exchanged with fresh medium supplemented with 15 μM PCB, incubated for 1 h in darkness and subsequently illuminated at 740 nm light, or at 660 nm for 1 h, or first at 660 nm (30 min) and subsequently at 740 nm (30 min) (all illuminations at 20 μmol m^{-2} s^{-1}, 1 h). After illumination, cells were fixed and analyzed by confocal microscopy. Scale bar, 5 μm. (d) Red light-inducible, far-red light-reversible nuclear localization of proteins. NIH/3T3 cells were cotransfected with expression vectors pMZ703 and pMZ725. Illumination and imaging was performed as in (c). Abbreviations: pA, polyadenylation signal; PCB, phycocyanobilin; P_{SV40}, simian virus 40 promoter.

expression of up to three transgenes by illuminating the cells with light of three different colors have been developed.[19−23]

Key to these optogenetic tools are protein-based photoreceptors that homodimerize or heterodimerize with specific binding partners in response to UV-B (UV-B receptor UVR8), blue (cryptochromes such as Cry2, or LOV-domains), green (Dronpa) or red (phytochromes such as the B-type, PhyB) light.[11,24,7,25] However, the reverse reaction is a spontaneous process with half-life times ranging from seconds to hours. This is determined by photobiological properties of the photoreceptors affecting the off kinetics upon the light-induced stimulus.[21,26] In the case of phytochromes, they cycle between their active (Pfr) and inactive (Pr) forms in a red/far-red light-dependent fashion. Red light (660 nm) drives conversion of PhyB into the Pfr-state (PfrB) and this conformer binds to phytochrome-interacting factors (PIFs). Far-red light (740 nm) reconverts the photoreceptor into its inactive state (PrB) and thereby induces dissociation from PIFs. This reversible photoswitch thus allows a fast on-command adjustment of signaling processes[8,19] and entails numerous potential advantages over blue light systems: a fine analogic quantitative adjustment of activity using ratios of red and far-red light, the inherent reversibility of the photoreceptor with switch-like characteristics, a highly resolved spatial resolution using combined red and far-red light patterns, as well as the lower toxicity and deeper tissue penetration of red light in comparison to light of shorter wavelengths.

DOI: 10.1021/acssynbio.5b00004
ACS Synth. Biol. 2015, 4, 951−958

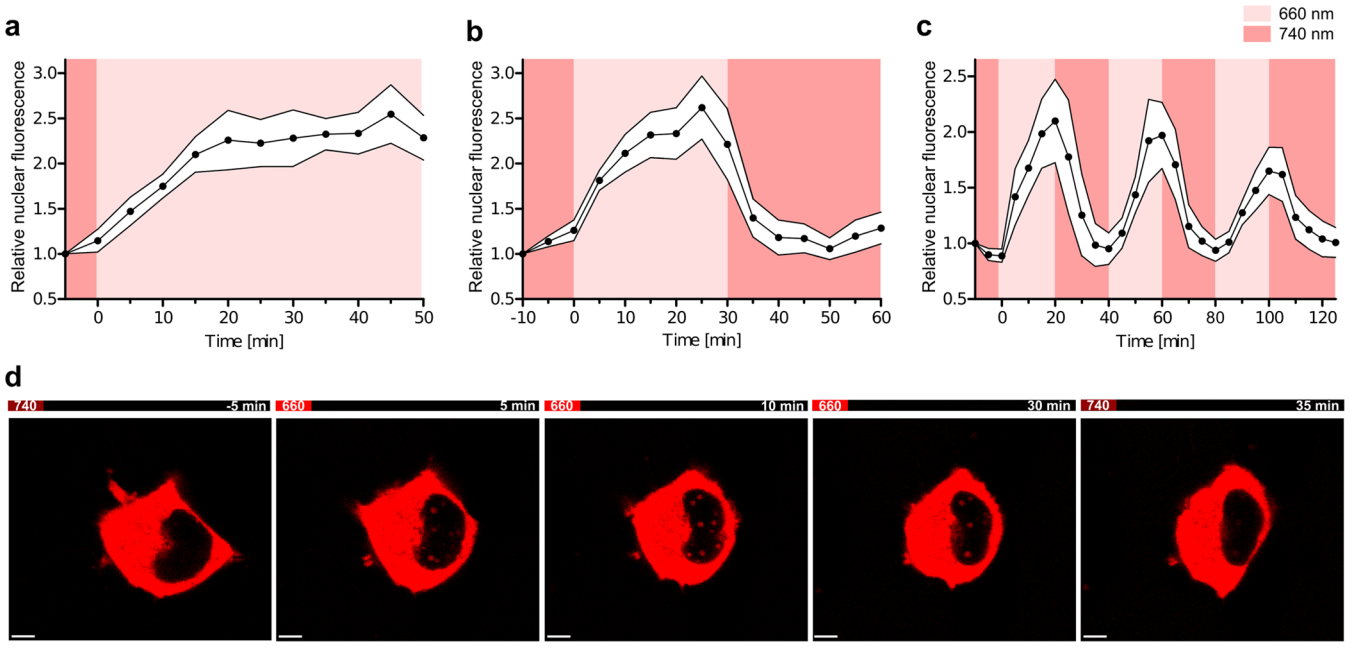

Figure 2. Kinetics of red light-induced nuclear import and far-red light-induced nuclear export by live cell imaging. (a–d) Plasmid pMZ703 encoding fluorescently labeled PhyB (1–908) with a C-terminally fused NES was cotransfected with plasmid pMZ725 encoding PIF3 into NIH/3T3 cells. Cells were incubated in the presence of 15 μM PCB under 740 nm light illumination for the indicated time spans until nuclear import was induced with 660 nm light at time point 0. The nuclear mean fluorescence intensity was followed with confocal microscopy time-lapse acquisitions. (a) Nuclear import was induced at 660 nm light for 50 min. n = 7. (b) The reversibility of nuclear import was monitored by sequential exposure of cells first to 660 nm light, followed by 740 nm (30 min, each). n = 5. (c) Multiple cycles of nuclear import and export were recorded over 125 min with import and export intervals of 20 min and the last interval 25 min. n = 11. (d) Microscope images of selected time points of one representative cell of (b). Scale bar, 5 μm. (a–c) Values were normalized to the first measurement of each group. Error boundaries represent one standard error of the mean.

In planta, PhyB transport into the nucleus upon red light illumination is essential for its biological activity. However, the exact mechanism mediating nucleo/cytoplasmatic partitioning of the photoreceptor is not yet fully understood.[27,28] Hypotheses include direct transport of PfrB upon the unmasking of nuclear localization sequence(s) under red light illumination[27] or, alternatively, an indirect transport mechanism that requires binding of PfrB to nuclear localization signal (NLS)-containing proteins such as PIF3.[28] We therefore evaluated whether these postulated transport mechanisms could be reconstructed in an orthogonal cellular platform, namely mammalian cells, to unravel the minimal molecular system involved in PhyB light-regulated subcellular localization. On the one hand, this novel experimental approach has shed light on the PhyB signaling mechanism active in plants in terms of PIF3 dependency for nuclear import following photoactivation. On the other hand, it has yielded a novel optogenetic tool for the spatiotemporally resolved control of signaling processes in nonplant systems relying on regulated nuclear transport. The optogenetic device developed in this work overcomes intrinsic limitations of existing optochemically[29] and blue light-regulated[15] systems. We show the dynamics and reversibility of nuclear import of proteins of interest in mammalian cell culture. Moreover, we introduce the first plant phytochrome-based optogenetic *in vivo* system implemented in vertebrates: this tool allows the spatiotemporal control of the nuclear localization of proteins, *e.g.*, transcription factors in zebrafish.

To reconstruct and assay plant phytochrome light-mediated nuclear import in mammalian cells, *Arabidopsis* phytochrome B (amino acids 1–908 containing the P1/NTE, P2/PAS, P3/GAF, P4/PHY, PAS-A and PAS-B domains) was fused to mCherry, while full-length *Arabidopsis* PIF3, encoding an intrinsic NLS, was fused to monomeric EGFP (mEGFP). On the basis of the PIF-mediated transport hypothesis,[28] this configuration should result in nuclear translocation of PhyB-mCherry and colocalization with PIF3-mEGFP under 660 nm illumination (Figure 1a). Both constructs were coexpressed in NIH/3T3 mouse fibroblasts supplemented with 15 μM of the chromophore phycocyanobilin (PCB) and exposed to 660 or 740 nm light (both at 20 μmol m^{-2} s^{-1}) for 1 h (Figure 1b,c). At 740 nm light, PhyB-mCherry was exclusively observed in the cytoplasm whereas illumination at 660 nm revealed PhyB-mCherry accumulation in the nucleus and colocalization with PIF3-mEGFP. Interestingly, PIF3-mEGFP formed discrete spots in the cell nucleus, which is in accordance with previous reports for PIF3 localization in plant nuclei.[30] The colocalization of PhyB-mCherry and PIF3-mEGFP was reverted by subsequent illumination at 740 nm, with PhyB-mCherry being homogeneously distributed in the nucleus (Figure 1c). The nuclear localization of PhyB-mCherry is strictly dependent on the presence of PIF3 and of PCB (Figure S1, Supporting Information).

Similar experiments employing full-length PhyB including its remnant C-terminal histidine kinase-related domain (HKRD) supported these findings (Figure S2a,b). Nuclear import of the full-length photoreceptor also depends on PIF3 indicating that regulated nucleo/cytoplasmatic partitioning of PhyB is not an intrinsic property of the photoreceptor itself.

If desired, exogenous addition of the chromophore, PCB, can be avoided by engineering mammalian cells for the biosynthesis of PCB as we have previously described.[31] Cotransfecting

DOI: 10.1021/acssynbio.5b00004
ACS Synth. Biol. 2015, 4, 951–958

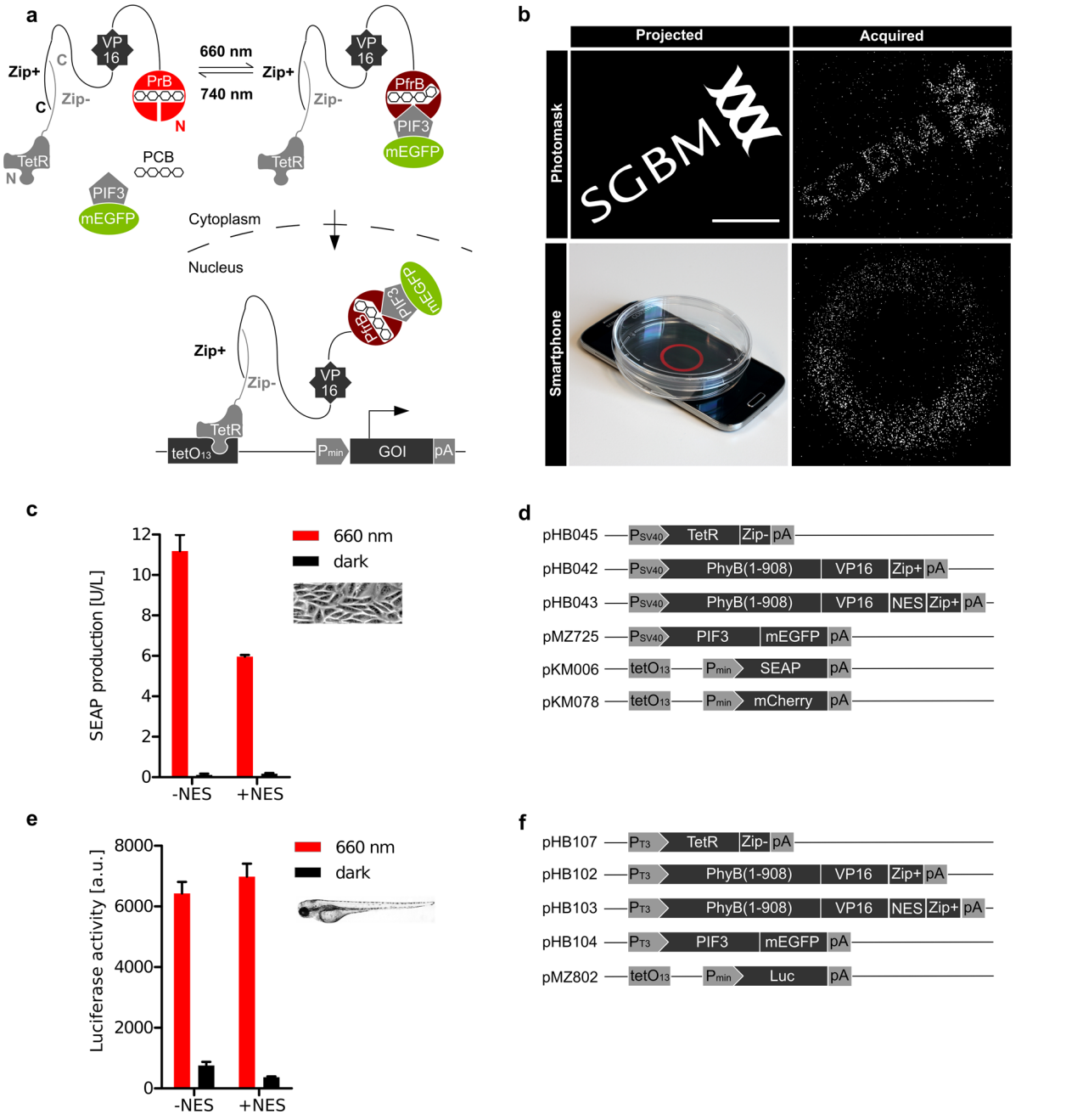

Figure 3. Spatially controlled, red light-inducible nuclear transport of transcription factors for controlling gene expression. (a) Design of the red light-inducible transcription factor transport. Phytochrome B (PhyB, amino acids 1−908) was fused to the *Herpes simplex* virus-derived activation domain VP16 and to one-half of a heterodimerizing antiparallel leucine zipper (Zip+). The DNA binding protein TetR was fused to the second half of the zipper (Zip−) leading to binding of both proteins. Upon coexpression of PIF3-mEGFP and illumination at 660 nm, the proteins are translocated into the nucleus where they activate gene of interest (GOI) expression from a minimal human cytomegalovirus promoter (P_{min}) fused to a 13-mer repeat of the TetR-specific operator tetO. (b) Spatial resolution of nuclear protein import. CHO-K1 cells were transfected with plasmids pHB045, pHB042, pMZ725 and pKM078 and illuminated through a photomask (3 h, 0.2 μmol m^{-2} s^{-1}) or were placed onto a smartphone screen projecting a circular pattern for 2.5 h (display brightness set to 15%). Post illumination, cells were incubated in the dark for 24 h prior to fixation and microscopic analysis. Scale bars, 1 cm. (c) Red light-inducible gene expression in Chinese hamster ovary (CHO-K1) cells. 70 000 CHO-K1 cells were seeded on glass coverslips in 24-wells and transfected after 24 h with plasmids pHB045, pHB042 (−NES)/pHB043 (+NES), pMZ725 and pKM006. Twenty-four hours post transfection, the medium was exchanged by fresh medium containing 15 μM PCB, and after 1 h cells were illuminated at 660 nm light (20 μmol m^{-2} s^{-1}) or kept in the dark for 48 h prior to quantifying SEAP production. n = 4, error bars represent one standard deviation of the mean. (d) Plasmids used in (b) and (c). (e) Red light-inducible gene expression in zebrafish. Single-cell stage embryos were injected with mRNA and the luciferase reporter plasmid. Twenty-one hours post fertilization, embryos were dechorionated and single larvae were incubated with 150 μM PCB for 2 h. Illumination with 660 nm light (20 μmol m^{-2} s^{-1}) was started subsequently, or the larvae were kept in the dark. After additional 2 h of illumination, *in vivo* luciferase activity was monitored in single fish embryos. n = 7−9, error bars represent one standard error of the mean, nonresponsive embryos resulting from an unsuccessful injection were identified statistically, as described elsewhere.[37] (f) Plasmids used in (e). Abbreviations: P_{T3}, T3 bacteriophage promoter. For further abbreviations, see Figure 1.

DOI: 10.1021/acssynbio.5b00004
ACS Synth. Biol. 2015, 4, 951−958

expression vectors for mitochondria-localized cyanobacterial heme oxygenase 1 (HO1) and PCB:ferredoxin oxidoreductase (PcyA)[31] (Figure S3) supported red light-inducible nuclear transport.

To obtain a tool for the dynamic control of nucleo/cytoplasmatic partitioning of PhyB, we rendered its natural nuclear import mechanism reversible. For this, PhyB-mCherry was fused to the nuclear export sequence (NES, MTKKFGTLTI) derived from the minute virus of mice. Upon coexpression of PhyB-mCherry-NES and PIF3-mEGFP in NIH/3T3 cells, 660 nm light-mediated nuclear transport of PhyB-mCherry-NES was observed while subsequent switching from 660 to 740 nm light induced export of the fusion protein into the cytoplasm (Figure 1b,d).

To further validate the functionality of the red light-inducible and far-red light-reversible nuclear translocation system, the dynamics were analyzed by confocal live-cell monitoring of the localization of the PhyB-mCherry-NES protein. First, protein import was followed after switching from preincubation at 740 to 660 nm light, thereby inducing nuclear import until saturation of the nuclear mean fluorescence intensity was reached (Figure 2a, Figure S4 and Movie S1). Maximal nuclear accumulation of the imported protein was repeatedly reached within 15 to 20 min after exposure to 660 nm red light. Next, we investigated the kinetics of nuclear export of the protein triggered by illumination with far-red light. To this aim, nuclear import in cells was first induced by illumination with 660 nm light for 30 min and then switching to 740 nm for another 30 min. A complete reversion of the nuclear import was observed after 5 to 10 min of far-red light exposure (Figure 2b,c,d and Movie S2). Finally, several cycles of nuclear import and export were recorded for 2 h with a duration of 20 min for each illumination period. In all cycles, nuclear accumulation of the protein was reversed to initial levels (Figure 2c). We noted that the maximal nuclear mean fluorescence measured in the first cycle decreased to ∼80% in the third cycle. The decrease is likely due to bleaching of the chromophore by the red light and laser used for excitation of mEGFP and mCherry. Photobleaching of the fluorescent protein is unlikely to be responsible for this effect, as it would also cause baseline drifting which was not observed.

As a proof of principle, we applied the red light-inducible, far-red light-reversible nuclear import system for the spatiotemporally resolved localization of transcription factors and gene expression in mammalian cells. To this end, we fused PhyB (amino acids 1−908) to the *Herpes simplex* virus-derived activation domain VP16 and to a heterodimerizing antiparallel leucine zipper[32] (Zip+). This zipper allows the recruitment of a DNA-binding protein of choice fused to a compatible zipper element (Zip−). Thus, attachment of the tetracycline repressor TetR to PhyB-VP16 resulted in a chimeric transcription factor. This complex was transported into the nucleus by PIF3-mEGFP upon 660 nm illumination and activated target promoters harboring TetR-specific tetO operator elements (Figure 3a). The introduction of the zipper pair will allow for the convenient exchange of the DNA-binding domain, providing a high degree of flexibility and versatility for potential combined applications with other gene expression systems.

Spatial control of signaling processes was achieved by transfection of this system into Chinese hamster ovary cells (CHO-K1). We demonstrated spatially resolved gene expression by locally illuminating CHO-K1 cells transfected with a red light-inducible expression cassette with mCherry as a reporter. For this purpose, we either placed a photomask between the 660 nm light source and the cell culture dish (Figure 3b upper panels) or cells were placed onto an AMOLED (active-matrix organic light-emitting diode) display of a mobile phone on which desired low-light patterns could simply be generated using a standard presentation software (Figure 3b, lower panels). The AMOLED display pixel size of 20 μm is in the size-range of a mammalian cell, thus providing a simple means of generating light patterns at cellular resolution. In both configurations, the projected light pattern was reproduced by the mCherry gene expression pattern, thus validating the suitability for spatially restricted nuclear transcription factor import (Figure 3b).

To functionally evaluate the performance of red light-induced nuclear import, the fluorescent reporter was exchanged for the human placental secreted alkaline phosphatase (SEAP) and the system was transfected transiently into CHO-K1 cells. Upon 660 nm illumination, a 95-fold increase in transgene expression levels was observed compared to the dark control. The addition of an NES motif to PhyB-VP16-Zip+ reduced maximum expression levels to 35-fold, likely due to a lower nuclear abundance of the transcription factor (Figure 3c,d). This red light-inducible gene expression system is further functional in NIH/3T3 mouse fibroblasts, in COS-7 African green monkey fibroblasts as well as in HEK-293T human embryonic kidney cells (Figure S5a). The system allows for reversible gene expression when reiteratively switching between 660 and 740 nm illumination (Figure S5b).

An *in vivo* implementation of this system in zebrafish was demonstrated by injecting expression vectors for PhyB-mCherry-NES and PIF3-mEGFP into single cell stage zebrafish embryos. At 33 h post fertilization (hpf), dechorionated embryos were placed in PCB-supplemented medium overnight prior to illumination with 660 nm light (20 μmol m^{-2} s^{-1}) for 1 h. In illuminated embryos, colocalization of both proteins was observed in the cell nucleus while embryos without PCB supplementation showed, as expected, only cytoplasmatic localization of PhyB-mCherry-NES (Figure S6a,b). Omitting the chromophore hence results in a system insensitive to light. Chromophore dependence thus provides, in this case, an experimental advantage: the setup of the phytochrome-based optogenetic *in vivo* system, namely injection/transfection, selection (of transgenics) and growth, can be conducted under ambient light conditions, as red light responsive nuclear transport occurs only after PCB addition. This feature represents an advantage over blue and green light-responsive systems which require safe-light illumination in order to avoid activation by accidental exposure to ambient light.

A more quantitative evaluation of the *in vivo* performance of red light-controlled nuclear protein import was achieved by injecting mRNA, encoding the gene expression system based on nuclear import together with a luciferase reporter plasmid, into zebrafish embryos. Dechorionated embryos at 24 and 48 hpf were soaked in medium containing 150 μM PCB for 2 h and were subsequently illuminated with 660 nm light for additional 2 h or kept in the dark before bioluminescence of single fish embryos was determined. The dependency on the NLS-harboring phytochrome interacting factor PIF3 and the chromophore PCB was validated *in vivo* (Figure S7c,d). A strong reporter expression was observed exclusively in 660 nm light illuminated fish (Figure 3e,f).

In this study, we have synthetically recapitulated the red light-inducible nuclear transport of truncated and/or full-length

DOI: 10.1021/acssynbio.5b00004
ACS Synth. Biol. 2015, 4, 951−958

Arabidopsis PhyB in mammalian cells and shown its dependence on the presence of PIF3. These experiments demonstrate that nuclear import of PhyB is not an intrinsic property of the photoreceptor itself, but relies on the presence of other factors including PIF3. This work, performed in a nonplant background, provides evidence in support of current hypotheses indicating that nuclear transport of PhyB can be mediated by PIF3 *in planta*. Not only does this validate the use of mammalian cells as an orthogonal platform for studying plant photoreceptor signaling processes, but furthermore, a highly valuable optogenetic tool has been developed for the spatiotemporally resolved manipulation of nuclear transport of proteins.

The approach presented here is complementary to methods developed to control (i) the nuclear accumulation[13,14] or (ii) regulate nuclear import[15] of proteins, and in addition it surpasses these in many aspects. For example, methods based on the passive accumulation of proteins in the nucleus are limited as these do not implicitly allow for the exclusion of target proteins from the nucleus. The red light-inducible nuclear transport system makes it feasible to have a protein excluded from the nucleus in the basal state and to trigger its shuttling in and out from the nucleus only upon illumination. This provides quantitative control of translocation of the target protein into and out of the nucleus, thus allowing precise assessment of its function or the induction of a signaling event.

Controlled light-induced nuclear transport of proteins has been demonstrated with LINuS, a tool employing the blue light-responsive LOV2 domain of *Avena sativa*.[15] Here exposure to blue light provokes the uncaging of an added NLS that is otherwise buried within the protein structure in the dark. The system benefits from its small size and is useful for triggering cellular processes, yet requires optimization (*e.g.*, reduce leakiness, increase dynamic range) for generalized applications. The optogenetic tool presented here based on the naturally evolved nuclear transport mechanism of PhyB is versatile and efficient. This red/far-red light regulated system overcomes inherent drawbacks of a blue light system, including toxicity at high light intensity, low tissue penetration and the requirement for constant protection from ambient light prior to the experiments. In addition, the switch-like behavior of the red/far-red light reversible system allows adjustable quantitative control either by manipulating the absolute light flux or the ratio between the intensities of both wavelengths. Moreover, this system makes it feasible to reduce background activation and/or achieve sharp patterns by simultaneous illumination with red and far-red light. Finally, the complementary characteristics of the red and blue light-inducible transport systems lead to the potential to develop novel, multiplexed applications by their combined use.

Optogenetic tools employing bacterial phytochromes utilizing a biliverdin chromophore have been successfully applied *in vivo*.[33−35] We implement here the first plant phytochrome-based optogenetic *in vivo* system in vertebrates by demonstrating red light-controlled nuclear protein import (and gene expression) in zebrafish. In this way, we further expand the toolbox of available optogenetic systems that might aid in understanding the mechanism and dynamics of cellular signaling processes in future research.

METHODS

Plasmids. The design and the construction of the expression vectors are described in Table S1.

Cell Culture and Transfection. Chinese hamster ovary cells (CHO-K1, ATCC CCL 61) were cultivated in HTS medium (Cell Culture Technologies) supplemented with 10% fetal calf serum (FCS, PAN, cat. no. 1502, batch P123002), 2 mM L-glutamine (Sigma), 100 U mL^{-1} penicillin and 0.1 mg mL^{-1} streptomycin (PAN). Mouse embryonic fibroblast cells (NIH/3T3, ATCC CRL-1658), human embryonic kidney cells (HEK-293T, ATCC CRL-11268), the African green monkey fibroblast-like cell-line COS-7 (ATCC CRL-1651), and human epitheloid cervix carcinoma HeLa cells (ATCC CCL-2) were maintained in Dulbecco's modified Eagle's medium (PAN, cat. no. P03−0710) supplemented with 10% FCS, 100 U mL^{-1} penicillin and 0.1 mg mL^{-1} streptomycin (PAN). For confocal imaging, cells were seeded onto glass coverslips placed in cell culture wells. For transfection, 70 000 cells (80 000 for COS-7) per well of a 24-well plate, or 3.5×10^6 cells per 10 cm Petri dish were transfected using polyethylenimine (PEI, linear, MW: 25 kDa, Polyscience) as described elsewhere[21] for transgene expression assays, or using *Trans*IT-X2 (Mirus Bio) for microscopy. The medium was exchanged 5 h post transfection. In cotransfections, all plasmids were applied in equal amounts (weight-based) except for the experiment for PCB biosynthesis (Figure S3), where the amount of pKM087 was doubled and transfection and subsequent cultivation being performed as described earlier.[31]

Light-Mediated Nuclear Transport. Twenty-four hours post-transfection, the cell culture medium was replaced by medium containing 15 μM PCB.[19] After chromophore addition, all steps were carried out under green safe-light (520 nm). Cells were subsequently incubated for 1 h in darkness in order to allow PhyB holoprotein assembly and were then illuminated with red or far-red light (660 or 740 nm, respectively) for the indicated time periods at a photon flux density of 20 μmol m^{-2} s^{-1}, unless indicated otherwise. Illumination was performed with LED panels emitting at 660 and 740 nm (Roithner, cat. No. LED660N-03, LED740_01 AU, respectively) with an electronic controller for adjusting light intensity. For smartphone-mediated nuclear transport, cells were seeded in a 10 cm dish, transfected and supplemented with PCB as described above and subsequently placed on the AMOLED display of a Samsung Galaxy S4 smartphone. Desired illumination patterns were generated using PowerPoint 2010 (Microsoft) and were displayed using Kingsoft Office 5.7.3 (Kingsoft Corporation) with an RGB red value of 255,0,0 and the display intensity set to 15%.

Analytics. SEAP production was quantified as described elsewhere.[36] For wide field microscopy analysis, cells were cultivated, transfected and illuminated in 10 cm dishes as described above. Cells were fixed with 4% paraformaldehyde (PFA, Roth) and mCherry production was analyzed with a BZ-9000 microscope (Keyence). Images were processed using ImageJ 1.47 (Gaussian Blur, brightness and contrast) and images were recolored from red to white using GIMP 2.8.4. For confocal imaging, illuminated cells on glass coverslips were washed once with ice cold DPBS with Ca^{2+}/Mg^{2+} (PAN) and subsequently fixed with 4% PFA for 10 min on ice followed by 10 min at room temperature. Cells were DAPI stained for 10 s in an aqueous DAPI solution (Roth, 1:5000 dilution of 1 mg mL^{-1} stock) and were washed with H_2O. Coverslips were embedded in Mowiol 4−88 (Roth) containing 15 mg mL^{-1} 1,4-diazabicyclo[2.2.2]octane (DABCO, Roth) and mounted onto glass microscope slides. Cells were imaged with a confocal microscope (Nikon Instruments Eclipse Ti-E with A1R

DOI: 10.1021/acssynbio.5b00004
ACS Synth. Biol. 2015, 4, 951−958

confocal laser scanner, 60× oil objective, NA = 1.49, or Nikon Instruments Eclipse Ni-E with a C2 confocal laser scanner, 60× oil objective NA = 1.40). mCherry, mEGFP and DAPI were visualized using excitation lasers of 561, 488, 405 nm and emission filters of 570−620, 500−550, 425−475 nm, respectively. Image acquisition, analysis and processing (brightness and contrast) were performed with NIS-Elements C (Nikon Instruments, version 4.10.04). For live-cell-imaging, cells on glass coverslips were washed once with DPBS with Ca^{2+}/Mg^{2+} at 37 °C and mounted on a coverslip holder with warm (37 °C) phenol red-free DMEM medium (PAN, cat. no. P04−01158) supplemented with 1% FCS and 4 mM L-glutamine. Before starting measurements, the recording medium was exchanged with fresh recording medium containing 15 μM PCB. Cells were illuminated with 740 nm light for 5−10 min for the PCB incorporation. Then, cells were exposed to different light and time conditions, as indicated. Measurements were carried out at 37 °C under green safe-light conditions. For the analysis of the nuclear import/export, images were only acquired using the mCherry channel. Nuclear localization was analyzed by normalizing the total mean fluorescence intensity of the nucleus, determined as regions of interest (ROI), over its starting value. ROIs were determined automatically for a given time series by using the Nikon software, and adjusted manually if necessary.

Zebrafish Experiments. Wild-type *Danio rerio* were raised under a 14/10 h light-dark cycle at ∼28.5 °C in a multitank recirculation system (Schwarz Ltd.) and fed commercial food and in-house hatched brine shrimp. Fertilized embryos were selected using a stereomicroscope (Leica Z2000, Nussloch) and single-cell stage embryos were injected with the respective plasmid DNA of 100 ng μL^{-1}, or mRNA of 25 ng μL^{-1} (total injection droplet 250−500 pL) produced using the mMESSAGE mMACHINE T3 Transcription Kit using a femtojet microinjector system (Eppendorf AG, Hamburg). Postinjection, embryos were raised at 28.5 °C and maintained in Petri dishes containing sterile E3 medium (5 mM NaCl, 0.17 mM KCl, 0.33 mM $CaCl_2$, 0.33 mM $MgSO_4$ in diethylpyrocarbonate (DEPC) water). At 21 h (luciferase assay) or 33 h (microscopy) postfertilization, embryos were dechorionated manually and then immediately dipped in E3 media containing 1% DMSO for 5 min at 21 h, or for 10 min at 45 h larval stages for 24 and 48 h measurements, respectively. For PCB treatment, embryos were transferred into wells containing fresh E3 medium supplemented with 150 μM PCB (E3 PCB).

For microscopy, embryos were kept in E3 medium postdechorionation and were then incubated in E3 PCB overnight and were next exposed to 660 nm light for 1 h (20 $\mu mol\ m^{-2}\ s^{-1}$). All experimental steps after PCB addition were performed under green safe-light (525 nm). After illumination, embryos were fixed in 4% PFA overnight and embedded in 0.7% low melting agarose for imaging. Confocal images were obtained using a Leica TCS SP5 X confocal laser-scanning microscope. Images were further processed (minimum intensity increased) using Imaris 6 (Bitplane AG).

For determining *in vivo* luciferase activity, embryos were kept for 2 h at 28.5 °C in E3 PCB and were subsequently exposed to 660 nm light (20 $\mu mol\ m^{-2}\ s^{-1}$) for additional 2 h. The medium was replaced by a solution containing E3 medium with 0.5 mM beetle luciferin (cat. no. L-8220, Biosynth). Plates were sealed with adhesive sealing sheets (cat. no. 6005185, TopSeal-A, PerkinElmer) and remained at 660 nm light for another 2 h, before bioluminescence was determined using an Envision Multilabel Plate Reader (PerkinElmer). Each well was measured immediately for 2.5 s. Nonresponsive embryos resulting from an unsuccessful injection were identified statistically, as described elsewhere.[37]

■ ASSOCIATED CONTENT

Supporting Information

Table S1, Figures S1−S7, Movies S1 and S2. This material is available free of charge *via* the Internet at http://pubs.acs.org.

■ AUTHOR INFORMATION

Corresponding Author

*E-mail: matias.zurbriggen@biologie.uni-freiburg.de.

Author Contributions

¶H.M.B., S.J., and K.H. contributed equally to this work.

Notes

The authors declare no competing financial interest.

■ ACKNOWLEDGMENTS

We thank Andreas Hiltbrunner (Freiburg, Germany) for kindly providing the plasmids 1858 pGAD24-PIF3 and 1930_pPPO43_phyB and Maximilian Ulbrich (Freiburg, Germany), and Kang Shen (Stanford, USA) for pGEMHE-XfA4-mEGFP and XW54_Punc_4c_NLS_Q, respectively. Imaging was supported by the light-imaging facilities at ZBSA and BIOSS. This work was supported by the Initiating and Networking Fund (IVF) of the Helmholtz Association within the Helmholtz Initiative on Synthetic Biology [SO-078], the European Research Council under the European Community's Seventh Framework Programme [FP7/2007−2013]/ERC [259043]-CompBioMat, EU IP ZF-HEALTH, the excellence initiative of the German Federal and State Governments [EXC 294-BIOSS, GSC 4-SGBM], BMBF Molecular Interaction Engineering (MIE), and the Interreg IV Upper Rhine program project number A20. W.R. was supported by a grant from the Ministry of Science, Research and the Arts of Baden-Württemberg (Az: 33−7532.20) and a starting grant of the European Research Council (Programme "Ideas", call identifier: ERC-2011-StG 282105).

■ REFERENCES

(1) Epstein, J. A., and Neel, B. G. (2003) Signal transduction: an eye on organ development. *Nature 426*, 238−239.

(2) Barry, E. R., Morikawa, T., Butler, B. L., Shrestha, K., de la Rosa, R., Yan, K. S., Fuchs, C. S., Magness, S. T., Smits, R., Ogino, S., Kuo, C. J., and Camargo, F. D. (2013) Restriction of intestinal stem cell expansion and the regenerative response by YAP. *Nature 493*, 106−110.

(3) Geisberger, R., Rada, C., and Neuberger, M. S. (2009) The stability of AID and its function in class-switching are critically sensitive to the identity of its nuclear-export sequence. *Proc. Natl. Acad. Sci. U. S. A. 106*, 6736−6741.

(4) Kau, T. R., Way, J. C., and Silver, P. A. (2004) Nuclear transport and cancer: from mechanism to intervention. *Nat. Rev. Cancer 4*, 106−117.

(5) Yang, W., Xia, Y., Ji, H., Zheng, Y., Liang, J., Huang, W., Gao, X., Aldape, K., and Lu, Z. (2011) Nuclear PKM2 regulates beta-catenin transactivation upon EGFR activation. *Nature 480*, 118−122.

(6) Beyer, H. M., Naumann, S., Weber, W., and Radziwill, G. (2014) Optogenetic control of signaling in mammalian cells. *Biotechnol. J. 10*, 273−283.

(7) Tischer, D., and Weiner, O. D. (2014) Illuminating cell signalling with optogenetic tools. *Nat. Rev. Mol. Cell Biol. 15*, 551−558.

DOI: 10.1021/acssynbio.5b00004
ACS Synth. Biol. 2015, 4, 951−958

(8) Levskaya, A., Weiner, O. D., Lim, W. A., and Voigt, C. A. (2009) Spatiotemporal control of cell signalling using a light-switchable protein interaction. *Nature 461*, 997−1001.
(9) Kennedy, M. J., Hughes, R. M., Peteya, L. A., Schwartz, J. W., Ehlers, M. D., and Tucker, C. L. (2010) Rapid blue-light-mediated induction of protein interactions in living cells. *Nat. Methods 7*, 973−975.
(10) Wend, S., Wagner, H. J., Muller, K., Zurbriggen, M. D., Weber, W., and Radziwill, G. (2013) Optogenetic Control of Protein Kinase Activity in Mammalian Cells. *ACS Synth. Biol. 3*, 280−285.
(11) Zhou, X. X., Chung, H. K., Lam, A. J., and Lin, M. Z. (2012) Optical control of protein activity by fluorescent protein domains. *Science 338*, 810−814.
(12) Chen, D., Gibson, E. S., and Kennedy, M. J. (2013) A light-triggered protein secretion system. *J. Cell Biol. 201*, 631−640.
(13) Yang, X., Jost, A. P., Weiner, O. D., and Tang, C. (2013) A light-inducible organelle-targeting system for dynamically activating and inactivating signaling in budding yeast. *Mol. Biol. Cell 24*, 2419−2430.
(14) Crefcoeur, R. P., Yin, R., Ulm, R., and Halazonetis, T. D. (2013) Ultraviolet-B-mediated induction of protein-protein interactions in mammalian cells. *Nat. Commun. 4*, 1779.
(15) Niopek, D., Benzinger, D., Roensch, J., Draebing, T., Wehler, P., Eils, R., and Di Ventura, B. (2014) Engineering light-inducible nuclear localization signals for precise spatiotemporal control of protein dynamics in living cells. *Nat. Commun. 5*, 4404.
(16) Usherenko, S., Stibbe, H., Musco, M., Essen, L. O., Kostina, E. A., and Taxis, C. (2014) Photo-sensitive degron variants for tuning protein stability by light. *BMC Syst. Biol. 8*, 128.
(17) Bugaj, L. J., Choksi, A. T., Mesuda, C. K., Kane, R. S., and Schaffer, D. V. (2013) Optogenetic protein clustering and signaling activation in mammalian cells. *Nat. Methods 10*, 249−252.
(18) Wu, Y. I., Frey, D., Lungu, O. I., Jaehrig, A., Schlichting, I., Kuhlman, B., and Hahn, K. M. (2009) A genetically encoded photoactivatable Rac controls the motility of living cells. *Nature 461*, 104−108.
(19) Müller, K., Engesser, R., Metzger, S., Schulz, S., Kampf, M. M., Busacker, M., Steinberg, T., Tomakidi, P., Ehrbar, M., Nagy, F., Timmer, J., Zubriggen, M. D., and Weber, W. (2013) A red/far-red light-responsive bi-stable toggle switch to control gene expression in mammalian cells. *Nucleic Acids Res. 41*, e77.
(20) Wang, X., Chen, X., and Yang, Y. (2012) Spatiotemporal control of gene expression by a light-switchable transgene system. *Nat. Methods 9*, 266−269.
(21) Müller, K., Engesser, R., Schulz, S., Steinberg, T., Tomakidi, P., Weber, C. C., Ulm, R., Timmer, J., Zurbriggen, M. D., and Weber, W. (2013) Multi-chromatic control of mammalian gene expression and signaling. *Nucleic Acids Res. 41*, e124.
(22) Müller, K., Engesser, R., Timmer, J., Zurbriggen, M. D., and Weber, W. (2014) Orthogonal optogenetic triple-gene control in Mammalian cells. *ACS Synth. Biol. 3*, 796−801.
(23) Müller, K., Naumann, S., Weber, W., and Zurbriggen, M. D. (2014) Optogenetics for gene expression in mammalian cells. *Biol. Chem. 396*, 145−152.
(24) Casal, J. J. (2013) Photoreceptor signaling networks in plant responses to shade. *Annu. Rev. Plant Biol. 64*, 403−427.
(25) Rizzini, L., Favory, J. J., Cloix, C., Faggionato, D., O'Hara, A., Kaiserli, E., Baumeister, R., Schafer, E., Nagy, F., Jenkins, G. I., and Ulm, R. (2011) Perception of UV-B by the *Arabidopsis* UVR8 protein. *Science 332*, 103−106.
(26) Ito, S., Song, Y. H., and Imaizumi, T. (2012) LOV domain-containing F-box proteins: light-dependent protein degradation modules in Arabidopsis. *Mol. Plant 5*, 573−582.
(27) Chen, M., Tao, Y., Lim, J., Shaw, A., and Chory, J. (2005) Regulation of phytochrome B nuclear localization through light-dependent unmasking of nuclear-localization signals. *Curr. Biol. 15*, 637−642.
(28) Pfeiffer, A., Nagel, M. K., Popp, C., Wust, F., Bindics, J., Viczian, A., Hiltbrunner, A., Nagy, F., Kunkel, T., and Schafer, E. (2012) Interaction with plant transcription factors can mediate nuclear import of phytochrome B. *Proc. Natl. Acad. Sci. U. S. A. 109*, 5892−5897.
(29) Engelke, H., Chou, C., Uprety, R., Jess, P., and Deiters, A. (2014) Control of protein function through optochemical translocation. *ACS Synth. Biol. 3*, 731−736.
(30) Ni, W., Xu, S. L., Chalkley, R. J., Pham, T. N., Guan, S., Maltby, D. A., Burlingame, A. L., Wang, Z. Y., and Quail, P. H. (2013) Multisite light-induced phosphorylation of the transcription factor PIF3 is necessary for both its rapid degradation and concomitant negative feedback modulation of photoreceptor phyB levels in Arabidopsis. *Plant Cell 25*, 2679−2698.
(31) Müller, K., Engesser, R., Timmer, J., Nagy, F., Zurbriggen, M. D., and Weber, W. (2013) Synthesis of phycocyanobilin in mammalian cells. *Chem. Commun. 49*, 8970−8972.
(32) Ghosh, I., Hamilton, A. D., and Regan, L. (2000) Antiparallel Leucine Zipper-Directed Protein Reassembly: Application to the Green Fluorescent Protein. *J. Am. Chem. Soc. 122*, 5658−5659.
(33) Gasser, C., Taiber, S., Yeh, C. M., Wittig, C. H., Hegemann, P., Ryu, S., Wunder, F., and Moglich, A. (2014) Engineering of a red-light-activated human cAMP/cGMP-specific phosphodiesterase. *Proc. Natl. Acad. Sci. U. S. A. 111*, 8803−8808.
(34) Ryu, M. H., Kang, I. H., Nelson, M. D., Jensen, T. M., Lyuksyutova, A. I., Siltberg-Liberles, J., Raizen, D. M., and Gomelsky, M. (2014) Engineering adenylate cyclases regulated by near-infrared window light. *Proc. Natl. Acad. Sci. U. S. A. 111*, 10167−10172.
(35) Folcher, M., Oesterle, S., Zwicky, K., Thekkottil, T., Heymoz, J., Hohmann, M., Christen, M., Daoud El-Baba, M., Buchmann, P., and Fussenegger, M. (2014) Mind-controlled transgene expression by a wireless-powered optogenetic designer cell implant. *Nat. Commun. 5*, 5392.
(36) Müller, K., Zurbriggen, M. D., and Weber, W. (2014) Control of gene expression using a red- and far-red light-responsive bi-stable toggle switch. *Nat. Protoc. 9*, 622−632.
(37) Jacobs, J. L., and Dinman, J. D. (2004) Systematic analysis of bicistronic reporter assay data. *Nucleic Acids Res. 32*, e160.

DOI: 10.1021/acssynbio.5b00004
ACS Synth. Biol. 2015, 4, 951−958